

## Z Pinch of a Gas Jet

J. Shiloh, A. Fisher, and N. Rostoker

*Physics Department, University of California, Irvine, California 92717*

(Received 3 October 1977)

A modified version of the vacuum spark experiment, in which a jet of argon is injected from the anode, is described. Experiments on a 1.26-kJ system have shown a strong pinching of the plasma with good reproducibility. The pinched plasma ( $\sim 20$  ns lifetime) is submillimeter in size with estimated temperature of 6–9 keV and density  $\geq 10^{18} e/cm^3$ . Advantages of such a device for the study of high-density plasmas and scaling up are discussed. Results are compared to vacuum spark and exploding wire experiments performed on the same system.

Z-pinch-produced plasmas of high density ( $\geq 10^{19} cm^{-3}$ ), and high temperature (a few keV) have been studied in three different experiments: dense plasma focus,<sup>1</sup> exploding wire,<sup>2</sup> and vacuum spark.<sup>3,4</sup> The main drawback in dense plasma focus experiments is the contact of the plasma with the wall causing restrikes which create serious limitations in efforts to scale up the input energy.<sup>5</sup> Exploding-wire and vacuum-spark plasmas do not come in contact with the wall, but the initial density is too high and too low, respectively, for proper implosion. This means that in the case of exploding wire one has to rely on the expansion of the vaporized wire at the beginning—before the wire material is ionized—and in the case of vacuum spark one has to rely on spark-created plasma from the electrodes' material to fill the gap before current can start to flow. As a result, vacuum-spark experiments are extremely irreproducible and exploding wires (unless exploded on very large machines with power of  $\geq 10^{12}$  W) do not produce to high temperatures because of large initial densities.

The device described in this Letter offers control over the initial density while the plasma is still kept away from the wall. Any gas can be used to form the plasma, so that both low- and high-Z ionic species can be studied on the same apparatus. The experiment can be fired repeti-

tively, and no conditioning is necessary.

The experimental setup is described in Fig. 1. A metallic vacuum chamber (pressure  $\sim 5 \times 10^{-6}$  Torr) contains a cone-shaped cathode and a flat anode with a 2.5-mm hole in the center. Both electrodes are made of graphite and the separation between them is  $\sim 8$  mm. A fast valve filled with argon gas at a pressure of  $\sim 4$  atm is activated and the gas flows through a nozzle and a diaphragm (the anode) to form a collimated jet between the two electrodes. At this point a 2.8- $\mu F$  capacitor bank charged to 30 kV is connected across the experiment via a high voltage switch. As a result, the gas breaks down and current starts to flow. The gas burst is sensed by a miniature spark gap, located below the nozzle, which breaks down when the gas front reaches it.

The combination of a fast valve,<sup>6</sup> a nozzle, and a diaphragm enables us to create a jet of gas with density of  $\sim 10^{17} cm^{-3}$  in a time shorter than 20  $\mu s$ . A measurement of the pressure rise as a function of time, using a fast ionization gauge,<sup>7</sup> is shown in Fig. 2. The size of the jet as determined from such measurements is 2.5 mm at the anode and  $\sim 4$  mm at the cathode. The collimation of the jet insures that the current starts to flow in a column between the two electrodes and the gas does

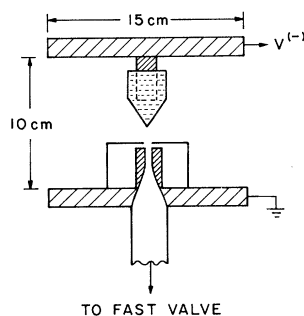


FIG. 1. Experimental setup, schematic.

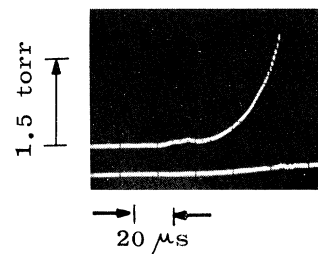


FIG. 2. Pressure risetime of the injected gas (using a fast ionization gauge). Top trace: ion current. Bottom trace: electron current. The density rises to  $10^{17} cm^{-3}$  in  $\sim 20 \mu s$ . The gauge is not calibrated at densities above  $10^{17} cm^{-3}$ .

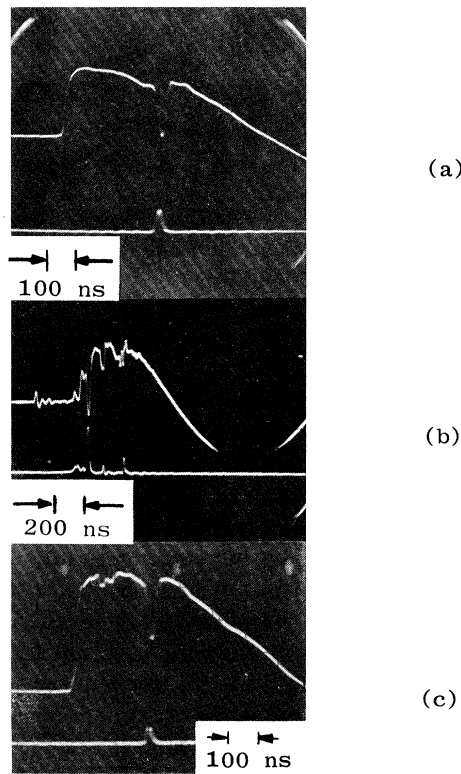


FIG. 3. Comparison of (a) puffed-gas, (b) vacuum-spark, and (c) exploding-wire experiments. Top trace measures  $dI/dt$  using a Rogovski coil and the bottom trace is the output of a  $p-i-n$  diode x-ray detector. (Vertical scales are arbitrary.)

not reach either the wall or the insulator.

The current in the system rises to 200 kA in 600 ns;  $\sim 300$  ns after the initial breakdown, a sharp drop in the rate of change of current simultaneously with a voltage spike and a burst of x rays ( $\sim 20$  ns) is observed [see Fig. 3(a)]. The above measurements (in addition to x-ray and visible-light photography) indicate a strong pinching of the plasma column. This result is reproducible, unlike the vacuum-spark case [see Fig. 3(b)], in the sense that one intense pinch is formed in every shot and the jitter in the time it occurs is  $\leq 50$  ns. The reproducibility is sensitive to the initial breakdown conditions; i.e., the electrodes' shape, the pressure rise time, and the delay between the valve's opening and the initial breakdown. Too short a delay will cause a behavior similar to the vacuum-spark case and too long a delay will cause a flashover along the insulator. The experiment can be fired repetitively without opening the vacuum system and with only a few minutes in between shots (limited by the time it

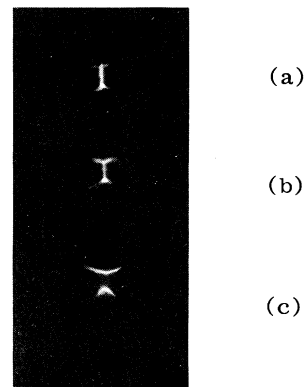


FIG. 4. Visible-light photography using a fast framing camera (10-ns exposure time). (a)  $t = 100$  ns, (b)  $t = 250$  ns (before the pinch), (c)  $t = 350$  ns after the pinch.

takes to evacuate the chamber after a shot). No conditioning of the system is necessary (probably because of the localization of the plasma away from the wall).

The collimated nature of the discharge is demonstrated in a set of pictures taken with a framing camera [see Fig. 4]. Figure 4(b) shows the plasma just before the pinch, and Fig. 4(c) was taken after the plasma column was disrupted. The electrodes' plasmas (as seen in Fig. 4) move toward each other at a speed of  $1.5$  cm/ $\mu$ s. The plasma radial velocity at the pinching stage is  $\sim 20$  cm/ $\mu$ s as measured from streak photography (see Fig. 5).

The shape and location of the pinched plasma were studied using x-ray pinhole photography (Fig. 6). The plasma appears to be elongated (along the anode-cathode axis) and its size varies from shot to shot between 0.1 and 0.25 mm in diameter and between 0.3 and 1.3 mm long. The location of the plasma is around the center of anode-cathode gap.

Two  $p-i-n$ -diode x-ray detectors with different

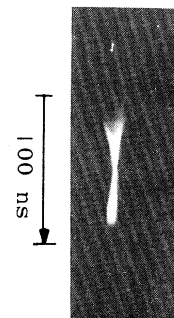


FIG. 5. Streak photograph. The split was 1 mm wide located at the midplane of the electrodes' spacing.

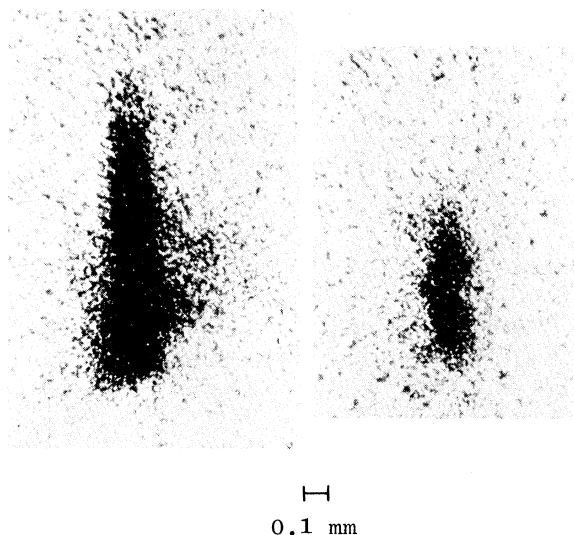


FIG. 6. X-ray pinhole photographs from two different shots. Pinhole diameter is  $20\ \mu\text{m}$ . Pinhole to source distance is 3 cm and pinhole to film distance is 1.5 cm.

foil absorbers have used to estimate the plasma electron temperature.<sup>8</sup> Absorbers include gold, nickel, and aluminum with thicknesses in the range of  $25\text{--}250\ \mu\text{m}$ . The temperatures all lie in the range of 6–9 keV. (Similar measurement for a vacuum-spark plasma gave  $\sim 30\ \text{keV}$ .) Using this temperature measurement, the plasma size as determined by x-ray pinhole photography, and the Bennett pinch relation, the electron density is found to be  $N_e \geq 10^{19}\ \text{cm}^{-3}$ .

The above measurement is just an estimate because of nonthermal effects. However, because all the foils gave similar results (6–9 keV), it is considered to be a good estimate.

Nonthermal effects that have been observed include the following: (a) High-energy x-rays ( $\geq 200\ \text{keV}$ ) were detected using a plastic-scintillator photomultiplier arrangement with 2-mm-thick lead absorber in front of it [see Fig. 7(a)]. (b) High-energy ions ( $\geq 200\ \text{keV}$ ) have been detected on a nitrocellulose film.<sup>9</sup> (c) When  $\text{D}_2$  was used instead of Ar the x-ray pulse on the scintillator-photomultiplier detector was followed by a pulse of neutrons ( $\sim 10^5$ ). At least part of them are believed to be of beam-target nature [see Fig. 7(b)].

Both vacuum-spark and exploding-wire experiments were performed on the same system, under the same conditions. Figure 3 compares results from the puffed-gas experiment to vacuum-

spark and exploding-wire experiments. In the vacuum-spark case, no external source of plasma prior to the application of high voltage was used, and a  $\sim 200\text{-ns}$  delay in the current rise is observed. (This delay corresponds to the time it takes for the electrodes' plasmas to fill the gap.) The behavior of the plasma is very erratic and nonreproducible (in agreement with other vacuum-spark experiments).<sup>10</sup>

In order to perform exploding-wire experiments the two electrodes were modified to hold a 6-mm-long,  $7\text{-}\mu\text{m}$ -diam graphite fiber (of comparable line density to that of the puffed-gas jet). The traces of current and x-ray measurements are reproducible and resemble those of the puffed-gas experiment. The initial heating, evaporation, and ionization of the wire take place during the first 10 ns.

Nonthermal effects, similar to the ones observed in the puffed-gas experiment were observed in vacuum-spark and exploding wire experiments.

The chain of events as inferred from the  $dI/dt$  trace, fast visible-light photography, and x-ray measurements is as follows: The injected jet of gas ( $\sim 10^{17}\ \text{cm}^{-3}$  density, 2.5 mm diameter at the bottom and  $\sim 4\ \text{mm}$  at the top) breaks down to form a plasma column. The plasma goes through

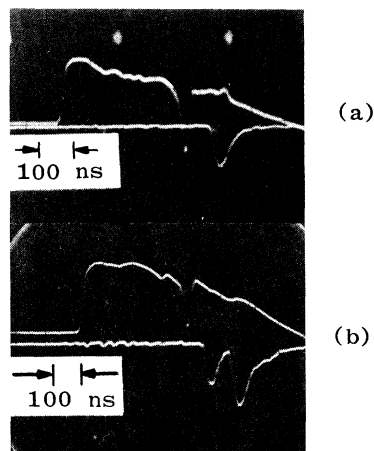


FIG. 7. High-energy x-rays and neutron measurements. The bottom trace is the output of a plastic-scintillator, photomultiplier system with 2-mm lead absorber in front of it, located 2 m from the experiment (a) with argon (b) with deuterium. (The delay between the time of the pinch and the x-ray pulse corresponds to electron collection time of the 12.5-cm-diameter photomultiplier. The long decay time is an inherent property of the photomultiplier.) The second pulse in (b) is due to a burst of neutrons emitted during the time of the pinch. Top trace measures  $dI/dt$ .

one or two "breathing motions" in which its collimated nature is retained and, after  $\sim 300$  ns, when the current reaches  $\sim 100$  kA, the plasma column pinches to form a localized submillimeter, hot (6–9 keV) plasma of density  $\geq 10^{19}e/cm^{-3}$ . The lifetime of the hot plasma is  $\sim 20$  ns. Afterwards, the plasma goes unstable, and no more pinches are observed.

The plasma produced in the puffed-gas device is of interest for further study because of its good reproducibility and compatibility with different gases, which makes it attractive for spectroscopic studies of x-rays emitted by highly ionized high- $Z$  elements such as argon, krypton, and xenon. The localization of the plasma away from the wall suggests good possibilities for the scaling up of the input energy.

This work was supported by the Defense Nuclear Agency.

<sup>1</sup>J. W. Mather, in *Methods of Experimental Physics*,

edited by Hans R. Griem and Ralph H. Lovberg (Academic, New York, 1971), Vol. 9, Pt. B., p. 187.

<sup>2</sup>P. G. Burkhalter, C. M. Dizier, and D. J. Nagel, Phys. Rev. A **15**, 700 (1977).

<sup>3</sup>T. N. Lie and R. C. Elton, Phys. Rev. A **3**, 875 (1971).

<sup>4</sup>J. L. Schwob and B. S. Fraenkel, Phys. Lett. **40A**, 81 (1972).

<sup>5</sup>J. W. Mather *et al.*, in *Proceedings of the Fourth International Conference on Plasma Physics and Controlled Nuclear Fusion Research, Madison, Wisconsin, 1971* (International Atomic Energy Agency, Vienna, Austria, 1972), Vol. 1, p. 561.

<sup>6</sup>A. Fisher, R. Mako, and J. Shiloh, to be published.

<sup>7</sup>E. A. Valsamakis, Rev. Sci. Instrum. **37**, 1318 (1966).

<sup>8</sup>R. C. Elton, Naval Research Laboratory Report No. 6738, 1968 (unpublished).

<sup>9</sup>Robert L. Fleischer, P. Buford Price, and Robert M. Walker, *Nuclear Tracks in Solids* (Univ. of California Press, Berkeley, Calif., 1975).

<sup>10</sup>J. Turechek, Ph.D. thesis, University of Maryland, 1972 (unpublished).

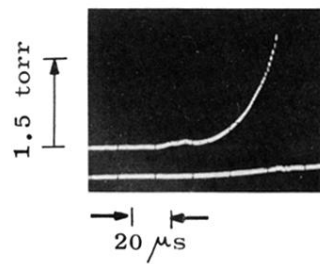


FIG. 2. Pressure risetime of the injected gas (using a fast ionization gauge). Top trace: ion current. Bottom trace: electron current. The density rises to  $10^{17} \text{ cm}^{-3}$  in  $\sim 20 \mu\text{s}$ . The gauge is not calibrated at densities above  $10^{17} \text{ cm}^{-3}$ .

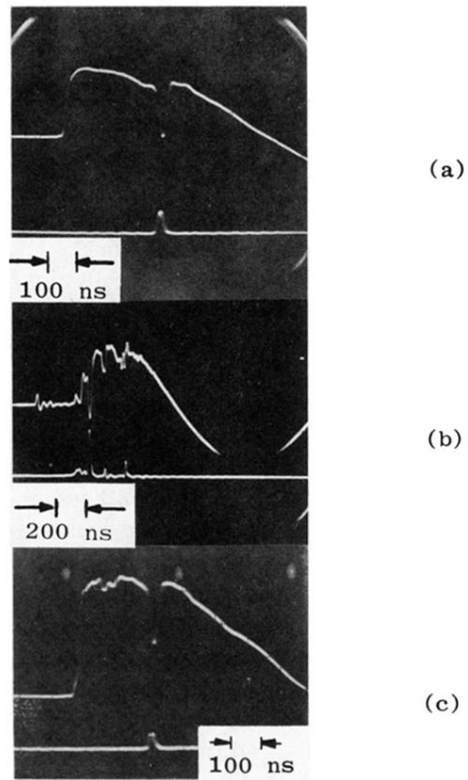


FIG. 3. Comparison of (a) puffed-gas, (b) vacuum-spark, and (c) exploding-wire experiments. Top trace measures  $dI/dt$  using a Rogovski coil and the bottom trace is the output of a  $p-i-n$  diode x-ray detector. (Vertical scales are arbitrary.)

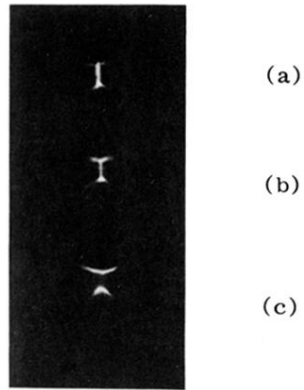


FIG. 4. Visible-light photography using a fast framing camera (10-ns exposure time). (a)  $t = 100$  ns, (b)  $t = 250$  ns (before the pinch), (c)  $t = 350$  ns after the pinch).

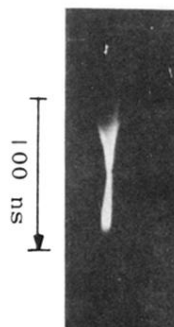
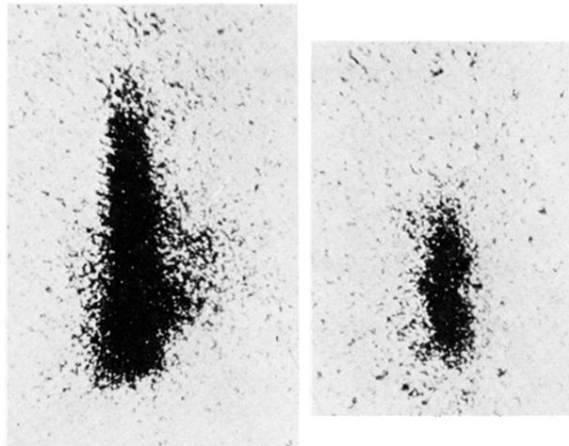


FIG. 5. Streak photograph. The split was 1 mm wide located at the midplane of the electrodes' spacing.





H  
0.1 mm

FIG. 6. X-ray pinhole photographs from two different shots. Pinhole diameter is  $20\ \mu\text{m}$ . Pinhole to source distance is 3 cm and pinhole to film distance is 1.5 cm.

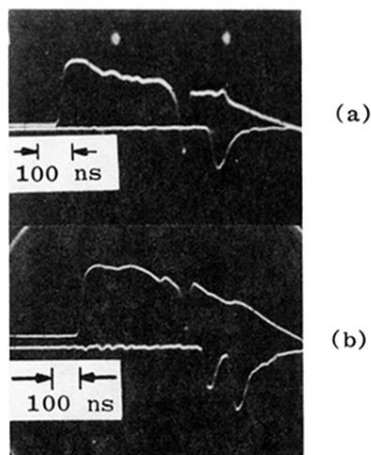


FIG. 7. High-energy x-rays and neutron measurements. The bottom trace is the output of a plastic-scintillator, photomultiplier system with 2-mm lead absorber in front of it, located 2 m from the experiment (a) with argon (b) with deuterium. (The delay between the time of the pinch and the x-ray pulse corresponds to electron collection time of the 12.5-cm-diameter photomultiplier. The long decay time is an inherent property of the photomultiplier.) The second pulse in (b) is due to a burst of neutrons emitted during the time of the pinch. Top trace measures  $dI/dt$ .